

## Immobilized Metal Affinity Chromatography (IMAC) of Mushroom Tyrosinase

Andrew Powell, undergraduate student, Indiana State University

Norman Siu, undergraduate student, Vincennes University

Jennifer K. Inlow, Assistant Professor, Indiana State University, [inlow@carbon.indstate.edu](mailto:inlow@carbon.indstate.edu)

William H. Flurkey, Professor, Indiana State University, [wflurkeyiii@isugw.indstate.edu](mailto:wflurkeyiii@isugw.indstate.edu)

### Abstract

Partially purified and crude commercial mushroom (*Agaricus bisporus*) tyrosinase was subjected to immobilized metal ion affinity chromatography (IMAC) with  $\text{Cu}^{2+}$ ,  $\text{Ni}^{2+}$ ,  $\text{Co}^{2+}$ , and  $\text{Zn}^{2+}$  metal ions bound to iminodiacetic acid (IDA) agarose. Under high salt conditions (500 mM NaCl) tyrosinase was retained on all immobilized metal IDA resins. In contrast, under low salt conditions (10 mM NaCl) tyrosinase was adsorbed only onto  $\text{Cu}^{2+}$  IDA agarose. Yields of recovered enzyme were high, and some of these IMAC resins removed contaminating proteins. The enzyme was also adsorbed onto  $\text{Cu}^{2+}$  DEAE columns under low salt conditions but not under high salt conditions. Although  $\text{Cu}^{2+}$  IDA columns have previously been used to purify polyphenol oxidases from a variety of plants sources, this is the first report of the use of other metal ions chelated to IDA to bind this enzyme, and it is the first report showing the effects of salt concentration on binding of this enzyme to IMAC resins.

### Introduction

Immobilized metal ion affinity chromatography (IMAC), also called metal chelate chromatography, has been used widely for purification of proteins since its introduction by Porath et al. [1] in 1975. Interactions of specific amino acid side chains, particularly those of histidine, cysteine, and tryptophan, with transition metal ions that are bound to the chelating groups of a chromatographic resin result in retention of proteins on the chromatographic column [for reviews see 2-8]. IMAC has been used to examine the relationship between amino acid side chain surface topography of proteins and binding selectivity [2]. One of the more recent applications of IMAC is the purification of recombinant proteins containing histidine tags [6, 8].

Tyrosinase (E.C. 1.14.18.1), also called polyphenol oxidase (PPO) in some species, is a copper-containing enzyme that catalyzes hydroxylation of monophenols and oxidation of diphenols in melanization and browning reactions in a variety of organisms [9]. Historically, the mushroom enzyme has been purified by adsorption or precipitation methods followed by ion exchange or size-exclusion chromatography. Most purifications of the enzyme have used anion-exchange chromatography followed by chromatography on hydroxyapatite. These methods can separate different isoforms of the enzyme. After Flurkey and Jen discovered that the enzyme can bind to Phenyl Sepharose through hydrophobic and affinity interactions [10, 11], chromatography on Phenyl Sepharose has been included in many purification schemes of the enzyme. In spite of the large number of reported purifications, tyrosinase still continues to be isolated in small amounts and often contains contaminants. In particular, commercial mushroom tyrosinase preparations, which have been used in numerous substrate and inhibition studies [12], contain many contaminants and may require extensive purification to obtain an enzyme sample free of other proteins [13]. IMAC could serve as an alternative purification method for removing some of the contaminating proteins in these tyrosinase preparations.

IMAC has already been used with some success in the purification or partial purification of PPO from artichokes [14], carrots [15], apples [16], and grapes [17]. In each of these examples,  $\text{Cu}^{2+}$  was immobilized on a chromatographic column by chelation with iminodiacetic acid (IDA) resin. Multiple peaks of enzyme were noted depending on the elution conditions, and multiple forms of

the enzyme were often present. For example, Richard–Forget et al. [16] have an extensive description of the purification of apple PPO using hydrophobic, affinity, and metal chelate chromatography (IMAC). In their study multiple peaks of the enzyme were observed after IMAC, but no clear separation of isoforms was noted. They concluded that ion-exchange chromatography was more selective than IMAC for separating PPO isoforms.

In a somewhat different approach, Wang et al. [18] purified tyrosinase from the skin of the white silky fowl in a single step using  $\text{Cu}^{2+}$  coordinated to the diethylaminoethyl group of DEAE cellulose. They concluded that retention of tyrosinase on the column was due to the formation of a tyrosinase -  $\text{Cu}^{2+}$  - DEAE complex. The complex was disrupted and the enzyme was eluted under acidic conditions. In a similar approach using  $\text{Cu}^{2+}$  DEAE chromatography, Liu et al. [19] purified a tyrosinase from *Bacillus thuringiensis*.

To explore the possibility that IMAC could remove protein contaminants from commercial mushroom (*Agaricus bisporus*) tyrosinase, we immobilized a variety of metal ions ( $\text{Cu}^{2+}$ ,  $\text{Ni}^{2+}$ ,  $\text{Co}^{2+}$ ,  $\text{Zn}^{2+}$ ) on IDA columns and tested their ability to separate tyrosinase from other protein contaminants.  $\text{Cu}^{2+}$  DEAE columns were also prepared and tested in a similar manner. Using the crystal structure of sweet potato catechol oxidase (CO) [20] as a template, a homology model for the structure of mushroom tyrosinase was developed and used to determine which amino acid residues might be available for binding to the immobilized metal ions.

## Experimental

**Materials.** Mushroom (*Agaricus bisporus*) tyrosinase, IDA agarose, and DEAE cellulose were obtained from Sigma (St. Louis, MO, USA). Mushroom tyrosinase was also purchased from Worthington Biochemical Corp. (Lakewood, NJ, USA). BCA (bicinchoninic acid) protein assays kits were obtained from Pierce Biotechnology Inc. (Rockford, IL, USA). All other chemicals were of reagent grade.

**Partial purification of mushroom tyrosinase.** Commercial mushroom tyrosinase was dissolved in buffer A (5 mM sodium phosphate, pH 6.0) at approximately 13 mg dry powder/mL buffer. One mL of the resuspension was applied to a 2 mL DEAE cellulose column equilibrated in buffer A. The column was washed with buffer A until the absorbance at 280 nm stabilized at the baseline level. Tyrosinase was then eluted with 30 mL of a 0-250 mM NaCl gradient in buffer A, followed by a 1 M NaCl wash in buffer A. Fractions were assayed for tyrosinase activity and subjected to SDS PAGE (see below) in order to ascertain tyrosinase purity. Based on enzymatic activity and the purity of tyrosinase in the fractions, selected fractions were pooled and dialyzed against 4 L of buffer B (10 mM MOPS, 10 mM NaCl, pH 7.0).

**IMAC using IDA columns.**

**Low salt conditions (10 mM NaCl):** Each mini-IDA column (ca 1.5 mL packed volume; 0.7 cm x 4 cm) was washed with water and then charged with 10 mL of one of the following metal ion solutions (6mg/mL, in water):  $\text{Cu(II)SO}_4 \cdot 5\text{H}_2\text{O}$ ,  $\text{Ni(II)SO}_4 \cdot 6\text{H}_2\text{O}$ ,  $\text{Co(II)SO}_4 \cdot 7\text{H}_2\text{O}$ ,  $\text{ZnSO}_4 \cdot 7\text{H}_2\text{O}$ . Each column was then washed with 15-20 mL of water followed by 15-20 mL of buffer B. One mL of the partially purified tyrosinase (see above) was applied, followed by 10 mL of buffer B. Tyrosinase was eluted by successive additions of 10 mL buffer B plus 10 mM glycine, 10 mL buffer B plus 100 mM glycine, and 10 mL buffer B plus 25 mM histidine. This was a modification of the procedure reported by Richard-Forget et al. [16]. 25 mM EDTA in buffer B was used to remove bound metal ions before recharging columns for further use. Note that some experiments omitted the 100 mM glycine elution step. All chromatography experiments were carried out at 22-23 °C.

**High salt conditions (500 mM NaCl):** Conditions were similar to those above except that 500 mM NaCl was included in the sample, equilibration buffer (10 mM MOPS, pH 7.0), and in all elution buffers containing 10 mM glycine, 25 mM histidine, or 25 mM EDTA. Similar experiments, under

both low and high salt conditions, were also carried out using crude commercial mushroom tyrosinase rather than the partially purified tyrosinase.

Cu<sup>2+</sup> DEAE chromatography. A 1% solution (w/v) of Cu(II)SO<sub>4</sub>·5H<sub>2</sub>O was prepared in deionized water. Concentrated ammonium hydroxide was added to the solution until the pH reached 9.5. DEAE cellulose was resuspended, washed with water, and then poured into a column (0.7 cm x 4 cm). The alkaline CuSO<sub>4</sub> solution was added to the DEAE cellulose column until the entire matrix was blue-green in color. The column was then equilibrated with buffer. Cu<sup>2+</sup> DEAE chromatography was carried out for partially purified and crude commercial mushroom tyrosinase under low salt (10 mM NaCl) and high salt (500 mM NaCl) conditions, using the equilibration conditions and elution buffers described above for IMAC with IDA columns.

Enzyme assays. Tyrosinase activity was monitored using modifications of previous procedures [21]. Each 1 mL assay contained 10 mM catechol in 100 mM sodium phosphate buffer at pH 6.5. Changes in absorbance at 410 nm were monitored over time. One unit of activity was defined as a change of one absorbance unit per min over the linear portion of the absorbance versus time curve.

SDS-PAGE. Sodium dodecyl sulfate polyacrylamide gel electrophoresis (SDS-PAGE) was carried out using the Laemmli system using precast (10-20% polyacrylamide) or in-house made (11% polyacrylamide) gels [22, 23]. Gels were dried between cellophane sheets and scanned to produce digital images.

Tyrosinase structure prediction by homology modeling. A structural model for mushroom tyrosinase was developed using the crystal structure of the sweet potato CO (PDB file 1BT3, [20]) as a template. The homology model was generated using the SWISS-MODEL server (<http://swissmodel.expasy.org>), Deep View Swiss-Pdb Viewer 3.7 (<http://www.expasy.org/spdbv/>; [24]), and a sequence alignment of the proteolyzed form (residues 1-360) of mushroom tyrosinase (UniProt accession number Q00024) with the proteolyzed form (residues 1-341) of sweet potato CO (UniProt accession number Q9ZP19). Figures showing protein structures were generated using Rasmol.

## Results

Commercial mushroom tyrosinase is sold as a brown-colored powder that is likely to contain organic material (presumably phenolic polymers), carbohydrates, and other proteins. The contaminating proteins vary in size from less than 14 kiloDaltons (kDa) to more than 100 kDa (Fig. 1, Cr). The tyrosinase in the commercial powder is a proteolyzed form (43-48 kDa) of the naturally occurring latent enzyme from live mushrooms (64 kDa) [9, 25, 26]. Because we were initially concerned that the colored material in the commercial powder could interfere with IMAC by binding to or displacing the immobilized metal ions, we first partially purified the enzyme by DEAE ion-exchange chromatography to remove the brown-colored compounds (Fig. 1). The pooled fractions from DEAE chromatography contained at least four low pI tyrosinase isoforms (pI 4.3-4.8) detectable by isoelectric focusing (data not shown). After using the partially purified enzyme for IMAC experiments, we also used the crude commercial tyrosinase without further purification in similar experiments to determine if the colored material interfered with IMAC (Table 1).

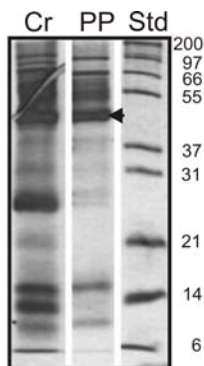


Fig.1. SDS-PAGE profile of commercial (Worthington) mushroom tyrosinase (Cr) and partially purified (PP) commercial mushroom tyrosinase. Cr: 42  $\mu\text{g}$  of commercial tyrosinase powder (12  $\mu\text{g}$  protein) was applied. PP: sample from pooled tyrosinase fractions (3  $\mu\text{g}$  protein) from DEAE cellulose chromatography was applied. Std: protein standards in kDa. Arrow indicates location of tyrosinase at  $\sim 45$  kDa.

Table 1

IMAC column	Partially purified tyrosinase			
	low salt		high salt	
	% nonbound	% bound	% nonbound	% bound
$\text{Cu}^{2+}$ IDA	0	67	0	81
$\text{Ni}^{2+}$ IDA	64	<1	0	79
$\text{Co}^{2+}$ IDA	64	<2	0	73
$\text{Zn}^{2+}$ IDA	61	<1	0	75
blank IDA	63	0	79	0
$\text{Cu}^{2+}$ DEAE	0	47	82	0

Crude tyrosinase				
	% nonbound	% bound	% nonbound	% bound
$\text{Cu}^{2+}$ IDA	0	83	0	74
$\text{Ni}^{2+}$ IDA	89	<2	<1	71
$\text{Co}^{2+}$ IDA	71	<1	24	47
$\text{Zn}^{2+}$ IDA	82	0	0	70
blank IDA	88	0	87	0
$\text{Cu}^{2+}$ DEAE	0	47	87	<2

Table 1. Recovery of tyrosinase from IMAC columns under low and high salt conditions. IMAC and enzyme activity determinations were carried out as described in the experimental section. Percentages refer to the amount of enzyme activity recovered in the bound or nonbound fractions relative to the total amount of enzyme activity applied to each column. Total recovery of enzyme activity is the sum of bound and nonbound enzyme activity.

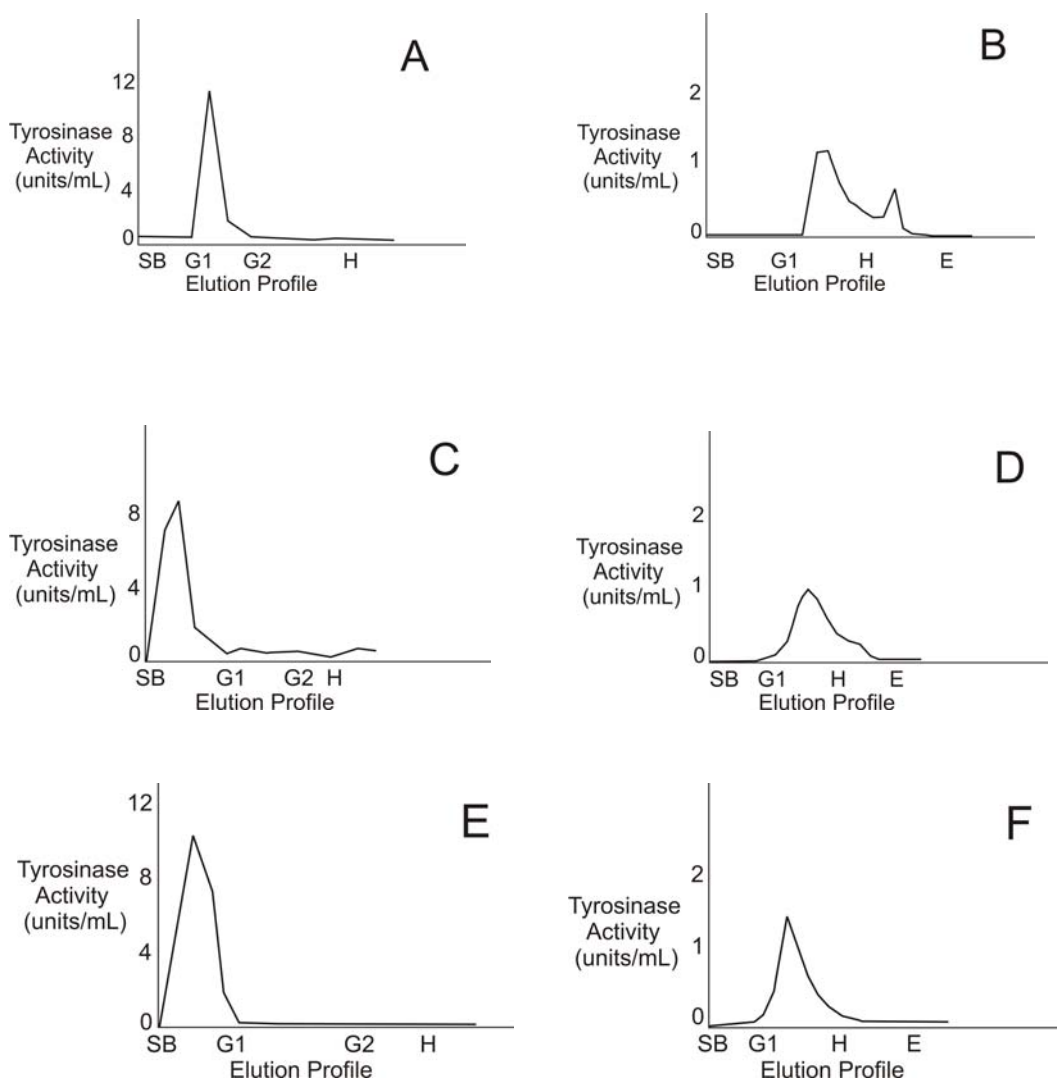
#### IMAC under Low Salt Conditions

Under low salt conditions (10 mM NaCl) partially purified mushroom tyrosinase was adsorbed onto  $\text{Cu}^{2+}$  IDA columns but not onto any of the other metal-IDA columns (Table 1). The enzyme was eluted from the  $\text{Cu}^{2+}$  IDA columns with 10 mM glycine in the buffer under these conditions (Fig. 2a). Higher concentrations of glycine and addition of histidine did not elute a significant amount of additional tyrosinase activity. Glycine and histidine in the buffer caused the elution of some of the  $\text{Cu}^{2+}$  ions from the column as evidenced by the pale blue color in the pooled glycine fractions and the dark blue color in the pooled histidine fractions, along with the loss of blue color from the column and an increase in absorbance at 280 nm. Under low salt conditions the enzyme was not adsorbed onto  $\text{Ni}^{2+}$  IDA,  $\text{Co}^{2+}$  IDA,  $\text{Zn}^{2+}$  IDA, nor blank (IDA without metal ions) columns (Table 1). Elution profiles of tyrosinase were similar for each of these four columns (Fig. 2c,e,g). Based on the color of the column and fractions collected, the glycine wash caused the

elution of some of the  $\text{Ni}^{2+}$  from the column, and the histidine wash caused the elution of  $\text{Ni}^{2+}$  and  $\text{Co}^{2+}$  ions from the columns. Using partially purified tyrosinase, total recovery of bound and nonbound enzyme ranged from 61 to 67% for the various IDA columns under low salt conditions. We could not estimate protein content in the bound and nonbound fractions in order to determine changes in specific activity of tyrosinase because of the small amount of protein applied to each column.

The chromatographic profiles of crude commercial tyrosinase under low salt conditions were very similar to those for partially purified tyrosinase under low salt conditions (chromatograms not shown). Total recovery of bound and nonbound enzyme under low salt conditions ranged from 71 to 89% (Table 1), higher than that using partially purified tyrosinase. Because no significant amount of enzyme was eluted with 100 mM glycine washes, this wash step was omitted for later IMAC experiments using high salt conditions. Approximately 500-600  $\mu\text{g}$  of total crude tyrosinase powder was applied to each of the columns. The protein content of this powder was estimated to be about 10% of the dry powder mass (data not shown).

Figure 2



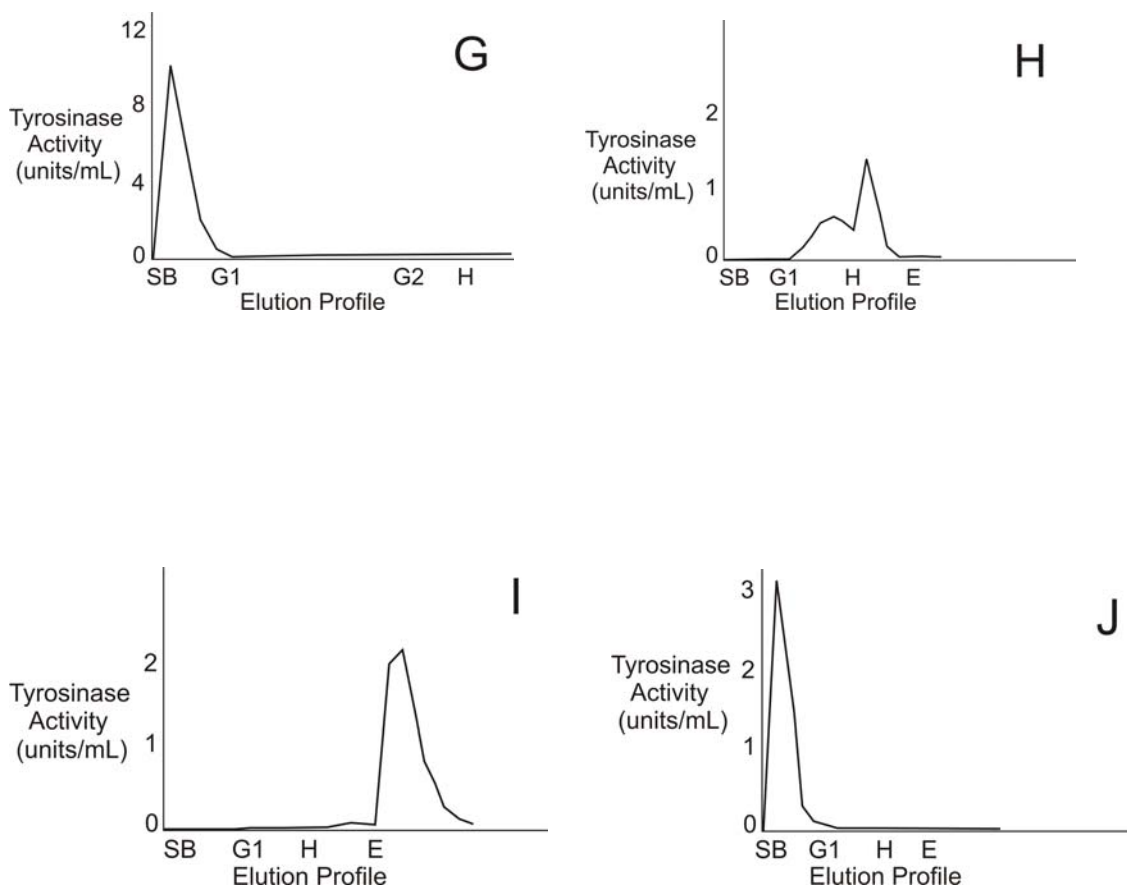


Fig. 2. Chromatography of partially purified tyrosinase on metal-IDA columns and  $\text{Cu}^{2+}$  DEAE columns.

(a)  $\text{Cu}^{2+}$  IMAC under low salt conditions. A  $\text{Cu}^{2+}$  IDA column was equilibrated with buffer B (10 mM MOPS, 10 mM NaCl, pH 7.0). Tyrosinase (ca 30  $\mu\text{g}$ ), partially purified by DEAE chromatography, was dialyzed against buffer B and applied to the column at S. At B, the column was washed with buffer B, at G1 with buffer B containing 10 mM glycine, at G2 with buffer B containing 100 mM glycine, and at H with buffer B containing 25 mM histidine.

(b)  $\text{Cu}^{2+}$  IMAC under high salt conditions. A  $\text{Cu}^{2+}$  IDA column (0.7x4 cm; ca 1.5 mL) was equilibrated with 10 mM MOPS buffer containing 500 mM NaCl at pH 7.0. Tyrosinase (ca 15  $\mu\text{g}$ ), partially purified by DEAE chromatography, was dialyzed against the equilibration buffer and applied to the column at S. At B, the column was washed with 10 mL buffer, at G1 with buffer containing 10 mM glycine, at H with buffer containing 25 mM histidine, and at E with buffer containing 25 mM EDTA.

(c)  $\text{Ni}^{2+}$  IMAC of partially purified tyrosinase under low salt conditions. Conditions for chromatography were as described in (a).

(d)  $\text{Ni}^{2+}$  IMAC of partially purified tyrosinase under high salt conditions. Conditions for chromatography were as described in (b).

(e)  $\text{Co}^{2+}$  IMAC of partially purified tyrosinase under low salt conditions. Conditions for chromatography were as described in (a).

(f)  $\text{Co}^{2+}$  IMAC of partially purified tyrosinase under high salt conditions. Conditions for chromatography were as described in (b).

(g)  $\text{Zn}^{2+}$  IMAC of partially purified tyrosinase under low salt conditions. Conditions for chromatography were as described in (a).

(h)  $Zn^{2+}$  IMAC of partially purified tyrosinase under high salt conditions. Conditions for chromatography were as described in (b).

(i)  $Cu^{2+}$  DEAE chromatography of tyrosinase under low salt conditions. Partially purified tyrosinase (ca 15  $\mu$ g) was dialyzed against buffer B and applied to a  $Cu^{2+}$  DEAE cellulose column equilibrated in buffer B at S. At B, the column was washed with buffer B, at G1 with buffer B containing 10 mM glycine, at H with buffer B containing 25 mM histidine, and at E with 25 mM EDTA.

(j)  $Cu^{2+}$  DEAE chromatography of tyrosinase under high salt conditions. Partially purified tyrosinase (ca 15  $\mu$ g) was dialyzed against 10 mM MOPS buffer containing 500 mM NaCl at pH 7.0 and applied to a  $Cu^{2+}$  DEAE cellulose column equilibrated in the same buffer (at S). At B, the column was washed with buffer, at G1 with buffer containing 10 mM glycine, at H with buffer containing 25 mM histidine, and at E with buffer containing 25 mM EDTA.

#### IMAC under High Salt Conditions

Under high salt conditions (500 mM NaCl) partially purified tyrosinase was adsorbed onto all IDA columns except the blank IDA column (Table 1). Elution from these columns required either glycine or histidine in the elution buffer (Fig. 2b, d, f, h). For the  $Cu^{2+}$ ,  $Ni^{2+}$ , and  $Zn^{2+}$  IDA columns multiple peaks of tyrosinase activity were apparent (Fig. 2b, d, h). Using partially purified tyrosinase, percent recovery of bound and nonbound enzyme under high salt conditions ranged from 73% to 81%, higher than the percentages recovered for partially purified tyrosinase under low salt conditions. Based on the color of the pooled fractions, it was apparent that the glycine washes caused the elution of some of the  $Cu^{2+}$  ions from  $Cu^{2+}$  IDA columns, and the histidine washes caused the elution of metal ions from  $Cu^{2+}$ ,  $Ni^{2+}$ , and  $Co^{2+}$  IDA columns.

The chromatographic profiles for crude commercial tyrosinase under high salt conditions on  $Cu^{2+}$ ,  $Ni^{2+}$ , and  $Zn^{2+}$  IDA columns were very similar to those for partially purified tyrosinase under high salt conditions on these columns (chromatograms not shown). In contrast, only 47% of the crude commercial tyrosinase applied to  $Co^{2+}$  IDA columns under high salt conditions was adsorbed to the column (Table 1); the remainder (24%) did not bind and eluted prior to the glycine wash (chromatogram not shown; see Table 1). When crude tyrosinase was applied to the various IDA columns under high salt conditions, the percent recovery of bound and nonbound enzyme ranged from 70-87%.

#### SDS-PAGE of IMAC Fractions

Following  $Cu^{2+}$  IMAC under low salt conditions, SDS-PAGE of the partially purified enzyme revealed that tyrosinase (45 kDa) was the major protein in the 10 mM glycine elution fractions, along with lesser amounts of other proteins with sizes in the ranges of 55-66 kD and 12-14 kDa (Fig. 3a). The 16 kDa protein present as a major contaminant in the crude commercial tyrosinase (Fig. 1) did not appear in any of the  $Cu^{2+}$  IMAC fractions. Similar protein contaminants were present in the tyrosinase-containing fractions from  $Ni^{2+}$  IMAC (Fig. 3b) except that there was a slightly greater amount of the 55 kDa protein present. SDS-PAGE profiles of fractions from  $Co^{2+}$  and  $Zn^{2+}$  IMAC (data not shown) were similar to that of  $Ni^{2+}$  IMAC.

Under high salt conditions two peaks of tyrosinase activity were eluted during  $Cu^{2+}$ ,  $Ni^{2+}$ , and  $Zn^{2+}$  IMAC of partially purified tyrosinase. SDS-PAGE of  $Cu^{2+}$  IMAC fractions revealed that contaminant proteins of 55 and 66 kDa were present along with tyrosinase (45 kDa) in the first peak of tyrosinase activity, while a 60 kDa protein was present with tyrosinase in the second peak (Fig. 3c). A similar protein profile was observed in the two peaks of tyrosinase activity from  $Ni^{2+}$  IMAC, except that the second peak contained more of the 60 kDa protein (Fig. 3c). SDS PAGE protein profiles for the pooled tyrosinase-containing fractions from  $Co^{2+}$  and  $Zn^{2+}$  IMAC (data not shown) were similar to those from  $Ni^{2+}$  IMAC.

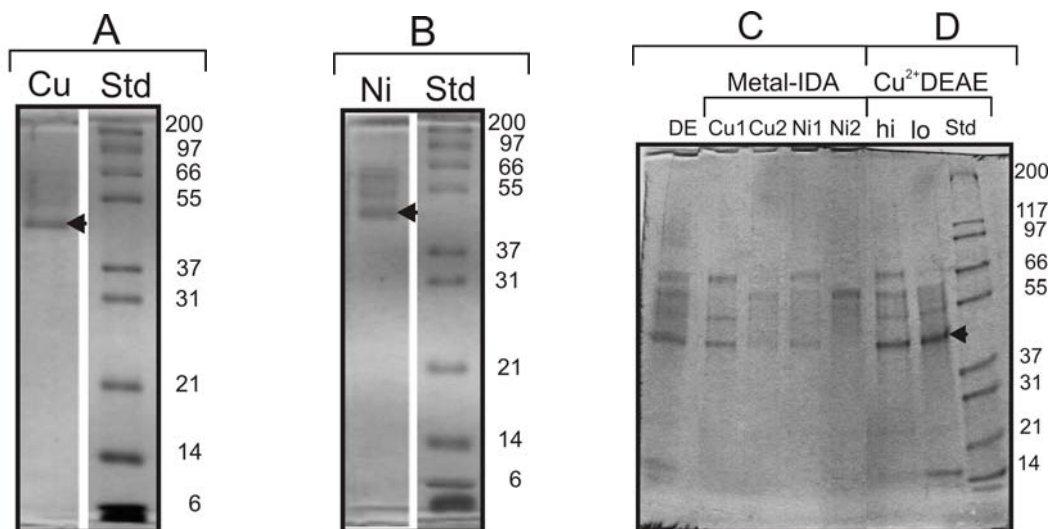


Fig. 3. SDS-PAGE of pooled fractions from metal-IDA and  $\text{Cu}^{2+}$  DEAE columns. In all cases, lanes labeled “Std” show protein standards and arrow heads indicate the position of tyrosinase at ~45 kDa.

- (a)  $\text{Cu}^{2+}$  IMAC under low salt conditions. Cu: bound tyrosinase fractions.  
 (b)  $\text{Ni}^{2+}$  IMAC under low salt conditions. Ni: nonbound tyrosinase fractions.  
 (c)  $\text{Cu}^{2+}$  and  $\text{Ni}^{2+}$  IMAC under high salt conditions. DE: partially purified tyrosinase from DEAE cellulose chromatography. Cu1: pooled tyrosinase fractions from first peak eluted from  $\text{Cu}^{2+}$  IDA column. Cu2: pooled tyrosinase fractions from second peak eluted from  $\text{Cu}^{2+}$  IDA column. Ni1: pooled tyrosinase fractions from first peak eluted from  $\text{Ni}^{2+}$  IDA column. Ni2: pooled tyrosinase fractions from second peak/shoulder eluted from  $\text{Ni}^{2+}$  IDA column.  
 (d)  $\text{Cu}^{2+}$  DEAE chromatography under high and low salt conditions. hi: pooled tyrosinase fractions from  $\text{Cu}^{2+}$  DEAE column under high salt conditions. lo: pooled tyrosinase fractions from  $\text{Cu}^{2+}$  DEAE column under low salt conditions.

#### $\text{Cu}^{2+}$ DEAE Chromatography

Partially purified tyrosinase was adsorbed onto  $\text{Cu}^{2+}$  DEAE columns under alkaline (pH 9.0) and neutral pH conditions. Following adsorption under alkaline conditions, tyrosinase was eluted by lowering the pH (pH 5.0) and increasing the ionic strength (addition of 1 M NaCl), but separation from other proteins was not achieved (data not shown). We also attempted to elute tyrosinase from  $\text{Cu}^{2+}$  DEAE columns with the succession of glycine and histidine-containing buffers used for the IDA columns. Under low salt conditions, the enzyme failed to elute from  $\text{Cu}^{2+}$  DEAE columns using the glycine and histidine elution buffers, and eluted only after the addition of buffer containing EDTA (Fig. 2i). Glycine and histidine caused the elution of some of the  $\text{Cu}^{2+}$  ions as evidenced by loss of color on the column, the faint blue color of the glycine fractions, and the dark blue color of the histidine fractions. The fractions from the EDTA wash had a faint blue color due to the removal of remaining  $\text{Cu}^{2+}$  ions. Recovery of the enzyme was relatively low (47%; Table 1) under low salt conditions. Pooled fractions of tyrosinase contained many of the contaminating proteins in the original sample (Fig. 3d). The contaminating proteins in these fractions were similar to those observed for tyrosinase eluted from DEAE columns without bound  $\text{Cu}^{2+}$  (compare Fig. 3d to Fig. 1).

Under high salt conditions the enzyme was not adsorbed onto the  $\text{Cu}^{2+}$  DEAE resin and the percentage of recovered enzyme was much greater than that under low salt conditions (82% using partially purified tyrosinase and 87% using crude commercial tyrosinase; Table 1, Fig. 2j). SDS-PAGE protein profiles of pooled tyrosinase fractions from  $\text{Cu}^{2+}$  DEAE columns under low

and high salt conditions were similar (Fig. 3d) except that there appeared to be smaller amounts of a 66 kDa protein in the tyrosinase fractions using low salt conditions.

#### Tyrosinase Structural Predictions

In order to ascertain which residues might be involved in the retention of mushroom tyrosinase on IMAC columns, a structural model of the proteolyzed form of mushroom tyrosinase (Fig. 4) was developed based on the enzyme's amino acid sequence homology to sweet potato CO, for which the crystal structure is available [20]. The proteolyzed form of mushroom tyrosinase (residues 1-360; UniProt accession number Q00024) contains a total of 13 histidine residues, 12 tryptophan residues, and one cysteine residue. Due to the hydrophobic nature of the tryptophan side chain, we expect all of the tryptophan residues to be largely buried when the enzyme is in the native state. According to our homology model, the single cysteine residue may be at least partially exposed. However, the sulfur atom of this cysteine is presumed to form a covalent thioether bond to a proximal histidine residue [26], as is the case for the corresponding cysteine residue in three homologous proteins: sweet potato CO [20], molluscan hemocyanin [27], and *Neurospora crassa* tyrosinase [28]. Six of the 13 histidine residues are located in the active site pocket and coordinated to the two active site  $\text{Cu}^{2+}$  ions (Fig. 4a). Two of the remaining seven histidine residues are presumed to be buried based on their locations in the homology model. The surface exposure of four other histidine residues is uncertain (Fig. 4a) because all four are located in or near regions of the mushroom tyrosinase sequence that are part of insertions or gaps in the sequence alignment used to generate the homology model. Mushroom tyrosinase and sweet potato CO share only ~20% amino acid identity. Therefore, we cannot confidently predict that any of these four residues is exposed and available for metal ion binding. The remaining histidine residue is the third residue from the N-terminus of the protein and is expected to be completely exposed, according to its location in the homology model (Fig. 4a, b).

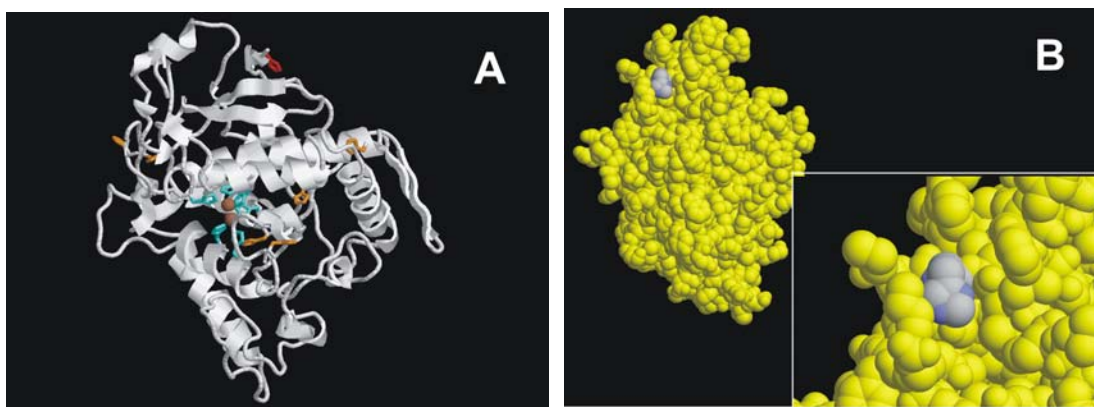


Fig. 4. Homology model for mushroom tyrosinase.

(a) Ribbon diagram of homology model for mushroom tyrosinase highlighting the side chains of the thirteen histidine residues. Blue: six active site histidine residues. Red: histidine residue that is expected to be exposed on the surface of the protein.

Orange: two histidine residues that are presumed to be buried, and four histidine residues for which surface exposure is uncertain. Brown spheres: two active site  $\text{Cu}^{2+}$  ions.

(b) Space-filling version of the homology model showing the location of the single histidine residue that is expected to be exposed on the surface of the protein. The molecule is rotated  $\sim 90^\circ$  clockwise relative to the molecule in (a). The histidine residue is shown in gray (carbon atoms) and blue (nitrogen atoms). The inset shows a close-up of the residue from the same orientation.

## Discussion

Although  $\text{Cu}^{2+}$  IDA columns have previously been used to purify PPO/tyrosinase from a variety of plants sources [14-17], this is the first report using other metal ions chelated to IDA to purify or characterize this enzyme. Chromatography of mushroom tyrosinase on all IMAC columns tested ( $\text{Cu}^{2+}$ ,  $\text{Ni}^{2+}$ ,  $\text{Co}^{2+}$ ,  $\text{Zn}^{2+}$ ) resulted in good recovery of active enzyme regardless of the identity of the metal ion. The recovery percentages were comparable to or larger than those reported for apple PPO [16], carrot PPO [15], and artichoke PPO [14] using  $\text{Cu}^{2+}$  IDA columns. The high recoveries of active enzyme suggest that IMAC may be useful for the purification of tyrosinases/PPOs from other species without a significant loss of enzyme activity.

Under low salt conditions, a single peak of tyrosinase activity was observed in all IMAC experiments; the enzyme was adsorbed onto  $\text{Cu}^{2+}$  IDA columns but not  $\text{Ni}^{2+}$ ,  $\text{Co}^{2+}$ , and  $\text{Zn}^{2+}$  IDA columns. This adsorption must be a result of tyrosinase binding to  $\text{Cu}^{2+}$  ions on the column since tyrosinase was not adsorbed onto blank IDA columns under low or high salt conditions. It has been shown that protein retention during IMAC is governed by histidine residues, and to a lesser extent cysteine and tryptophan residues, exposed on the surface of a protein interacting with the immobilized metal ions [4, 6, 8]. Histidine residues, in the unprotonated state, have the highest affinity for  $\text{Cu}^{2+}$  IDA resin, followed by reduced cysteine residues, followed by tryptophan residues [4]. A single histidine residue on the surface of a protein is sufficient for weak binding to  $\text{Cu}^{2+}$  IDA resin, but multiple proximal histidines are necessary for binding to  $\text{Zn}^{2+}$  or  $\text{Co}^{2+}$  IDA resin [6]. The adsorption behavior we observed suggests that under low salt conditions there is at least one exposed histidine residue, allowing binding to  $\text{Cu}^{2+}$  IDA columns, but not multiple exposed histidine residues since the enzyme did not bind to  $\text{Ni}^{2+}$ ,  $\text{Co}^{2+}$ , or  $\text{Zn}^{2+}$  IDA columns. The histidine that is the third residue from the N-terminus of the protein (Fig. 4a, b), which is expected to be exposed on the protein's surface, is the residue most likely to be responsible for retention of tyrosinase on  $\text{Cu}^{2+}$  IDA columns although we can not rule out binding to some of the other histidine residues. One might predict that the two active site  $\text{Cu}^{2+}$  ions coordinated to the six active site histidine residues could potentially become coordinated to free IDA groups on the resin. However, based on the enzyme's weak binding to  $\text{Cu}^{2+}$  IDA columns (elution with low glycine concentration), it appears the six active site histidine residues are not involved in retention, possibly because the IDA group is too bulky to fit into the active site pocket with the proper orientation for coordination to the active site  $\text{Cu}^{2+}$  ions.

We carried out IMAC under high salt conditions to determine if electrostatic interactions played a role in the retention of tyrosinase on IDA resins. Under high salt conditions, which should have eliminated these interactions, tyrosinase was adsorbed onto  $\text{Cu}^{2+}$ ,  $\text{Ni}^{2+}$ ,  $\text{Co}^{2+}$ , and  $\text{Zn}^{2+}$  IDA columns. The most likely explanation for the change in binding behavior relative to low salt conditions is that the higher salt concentration is affecting the protein structure. As a result more histidine, tryptophan, and/or cysteine residues presumably become exposed on the protein's surface, allowing binding to  $\text{Ni}^{2+}$ ,  $\text{Co}^{2+}$ , and  $\text{Zn}^{2+}$  IDA columns. This finding of a change in binding behavior dependent on salt concentration suggests that strategies for purifying tyrosinase from a variety of species could be developed using different metal ions and a range of salt concentrations to achieve the desired binding or elution behavior. If an increase in salt concentration during IMAC indeed causes structural changes in mushroom tyrosinase, similar structural changes in the enzyme may also occur during ion exchange chromatography (IEC) which is commonly used to purify the enzyme. An increase in salt concentration during IEC may result in exposure of more positively and/or negatively charged amino acid side chains in the enzyme that could affect binding to or elution from the ion exchange resin. Additional experiments are needed to determine if structural changes in the enzyme are in fact occurring as a result of exposure to high salt concentrations.

Reports describing  $\text{Cu}^{2+}$  IMAC for apple [16], grape [17], artichoke [14], and carrot [15] PPO used 100 mM KCl, 150 mM NaCl, 150 mM NaCl, and 200 mM NaCl in their equilibration/elution buffers, respectively. Elution profiles for apple, grape, and artichoke PPOs showed multiple peaks of eluted enzyme, some of which were adsorbed and some of which were not. The salt

concentrations used in these earlier studies are intermediate between the low (10 mM) and high (500 mM) salt concentrations used in this study. We speculate that the salt concentrations used in these earlier studies may have led to changes in the structure of subsets of PPO molecules, resulting in the elution of multiple peaks of enzyme, similar to what we observed for mushroom tyrosinase under high salt conditions. This hypothesis is also supported by the observation of Richard-Forget et al. that IMAC did not separate isozymes of tyrosinase; multiple peaks were eluted, but each peak contained multiple isozymes [16].

Wang et al. provided evidence for the involvement of  $\text{Cu}^{2+}$  in the retention of tyrosinase from the white silky fowl on  $\text{Cu}^{2+}$  DEAE resin [18]. In our experiments mushroom tyrosinase was retained on  $\text{Cu}^{2+}$  DEAE columns at pH 7 under low salt conditions (Fig. 2i); it was not eluted when glycine and histidine were added to the buffer, but was eluted only when the column was washed with EDTA which disrupts the  $\text{Cu}^{2+}$ -DEAE complex. In contrast, under high salt conditions at pH 7, mushroom tyrosinase did not bind to  $\text{Cu}^{2+}$  DEAE columns (Fig. 2j). Furthermore, the enzyme eluted from  $\text{Cu}^{2+}$  DEAE columns at this pH using a NaCl gradient (data not shown). From these data it appears that the retention of mushroom tyrosinase on  $\text{Cu}^{2+}$  DEAE resin under low salt conditions is due primarily to ionic interactions with free DEAE functional groups, rather than interaction with the  $\text{Cu}^{2+}$  ions immobilized on the column. Presumably, some fraction of DEAE groups did not have bound  $\text{Cu}^{2+}$  ions (i.e., the column was not completely saturated with  $\text{Cu}^{2+}$ ), and these groups, when protonated, could interact with negatively charged side chains on the surface of the enzyme. The use of a high salt concentration in the buffer appears to eliminate these ionic interactions so that tyrosinase does not bind to the column. In related experiments mushroom tyrosinase did not elute from regular DEAE columns (without bound  $\text{Cu}^{2+}$ ) at pH 7 and low salt concentration using buffers containing glycine or histidine, but only eluted with the addition of EDTA to the buffer (data not shown). This indicates that EDTA eluted tyrosinase from DEAE resin by ion exchange interactions. This phenomenon probably led to the elution of tyrosinase from  $\text{Cu}^{2+}$  DEAE resin under low salt conditions (Fig. 2i). Whether under high or low salt conditions,  $\text{Cu}^{2+}$  DEAE chromatography did not provide an advantage in terms of enzyme purification over regular DEAE ion exchange chromatography because the pattern of contaminating proteins after chromatography was similar in both cases (compare Fig. 1 to Fig. 3d).

It is clear from SDS-PAGE analysis of the IMAC fractions that some IMAC columns can selectively remove certain contaminating proteins from partially purified or crude commercial mushroom tyrosinase. Specifically, the  $\text{Ni}^{2+}$ ,  $\text{Co}^{2+}$ , and  $\text{Zn}^{2+}$  IDA columns did not retain tyrosinase under low salt conditions, but other proteins of higher or lower molecular weight were adsorbed. In contrast, tyrosinase was adsorbed onto  $\text{Cu}^{2+}$  IDA columns under low salt conditions while some of the contaminating proteins were not. Thus, IMAC can be a useful component in the purification of mushroom tyrosinase and, potentially, the purification of PPO/tyrosinase from other organisms.

## Conclusion

Mushroom tyrosinase was adsorbed onto  $\text{Cu}^{2+}$  IDA resins under low salt and high salt conditions, but was only retained on  $\text{Ni}^{2+}$ ,  $\text{Co}^{2+}$ ,  $\text{Zn}^{2+}$  IDA resins under high salt conditions. Therefore, tyrosinase binding in IMAC is dependent on the type of metal ion and salt concentration used. Binding to IMAC resins is presumed to be mediated by one or more histidine residues exposed on the surface of the protein. Binding of tyrosinase to  $\text{Cu}^{2+}$  DEAE resins appeared to be primarily through ionic interactions and not through metal affinity coordination.

## References

1. Porath J, Carlsson J, Olsson I, Belfragge G. Metal chelate affinity chromatography, a new approach to protein fractionation. *Nature*. 1975; 258:598-599.
2. Fatiadi AJ. Affinity chromatography and metal chelate affinity chromatography. *Crit Rev Anal Chem*. 1987; 18:1-44.

3. Porath J. Amino acid side chain interaction with chelate-liganded crosslinked dextran, agarose, and TSK-gel, A mini review of recent work. *J Mol Recognit.* 1990; 3:123-124.
4. Porath J, Immobilized metal ion affinity chromatography. *Protein Expr Purif.* 1992; 3:263-281.
5. Kågedal L. Immobilized Metal Ion Affinity Chromatography. In: Janson J-C, Rydén L, eds. *Protein Purification: Principles, High-Resolution Methods, and Applications.* 2<sup>nd</sup> ed. New York: John Wiley & Sons, Inc.; 1998:311-342.
6. Gaberc-Porekar V, Menart V. Perspectives of immobilized-metal affinity chromatography. *J Biochem Biophys Methods.* 2001; 49:335-360.
7. Mrabet NT, Vijayalakshmi MA. Immobilized Metal-Ion Affinity Chromatography: From Phenomenological Hallmarks to Structure-Based Molecular Insights. In: Vijayalakshmi MA, ed. *Biochromatography: Theory and Practice.* London: Taylor & Francis, Ltd.; 2002:272-294.
8. Ueda EKM, Gout PW, Morganti L. Current and prospective applications of metal ion-protein binding. *J Chromatogr A.* 2003; 988:1-23.
9. van Gelder CWG, Flurkey WH, Wichers HJ. Sequence and structural features of plant and fungal tyrosinases. *Phytochemistry.* 1997; 45:1309-1323.
10. Flurkey WH, Jen JJ. Peroxidase and polyphenol oxidase activities in developing peaches. *J Food Sci.* 1978; 43:1826-1828.
11. Flurkey WH, Jen JJ. Hydrophobic adsorption chromatography of peach polyphenol oxidase. *J Food Sci.* 1980; 45:1622-1624.
12. Seo SY, SharmaVK, Sharma N. Mushroom tyrosinase: recent prospects. *J Agric Food Chem.* 2003; 51:2837-2853.
13. Kumar M, Flurkey WH. Activity, isoenzymes, and purity of mushroom tyrosinase in commercial preparations. *Phytochemistry.* 1991; 30:3899-3902.
14. Zawistowski J, Weselake RJ, Blank G, Murray ED. Fractionation of Jerusalem artichoke phenolase by immobilized copper affinity chromatography. *Phytochemistry.* 1987; 26:2905-2907.
15. Söderhäll I, Söderhäll K. Purification of prophenol oxidase from *Daucus carota* cell cultures. *Phytochemistry.* 1989; 28:1805-1808.
16. Richard-Forget F, Goupy P, Nicolas J. New approaches for separating and purifying apple polyphenol oxidase isoenzymes: hydrophobic, metal chelate and affinity chromatography. *J Chromatogr A.* 1994; 667:141-153.
17. De Stafano G, Piacquadio P, Sciancalepore V. Fractionation of grape polyphenoloxidase by immobilized copper affinity chromatography. *Riv Vitic Enol.* 1996; 49:69-76.
18. Wang H, Liu W, Ulbrich N. Isolation and characterization of a tyrosinase from the skin of the white silky fowl (*Gallina lanigera*) employing copper saturated diethylaminoethyl-cellulose. *Biochim Biophys Acta.* 1995; 1243:251-255.
19. Liu N, Zhang T, Wang YJ, Huang YP, Ou JH, Shen P. A heat inducible tyrosinase with distinct properties from *Bacillus thuringiensis*. *Lett Appl Microbiol.* 2004; 39:407-412.
20. Klabunde T, Eicken C, Sacchetti JC, Krebs B. Crystal structure of a plant catechol oxidase containing a dicopper center. *Nat Struct Biol.* 1998; 5:1084-1090.
21. Zhang X, Flurkey WH. Purification and partial characterization of tyrosinase isoforms from cap flesh of Portabella mushrooms. *Journal of Food Biochemistry.* 1999; 23:95-108.
22. Fan Y, Flurkey WH. Purification and characterization of tyrosinase from gill tissue of Portabella mushrooms. *Phytochemistry.* 2004; 65:671-678.
23. Chen L, Flurkey WH. Effect of protease inhibitors on the extraction of Crimini mushroom tyrosinase isoforms. *Current Topics in Phytochemistry.* 2002; 5:109-120.
24. Guex N, Peitsch MC. SWISS-MODEL and the Swiss-PdbViewer: an environment for comparative protein modeling. *Electrophoresis.* 1997; 18:2714-2723.
25. Espín JC, van Leeuwen J, Wichers HJ. Kinetic study of the activation process of a latent mushroom (*Agaricus bisporus*) tyrosinase by serine proteases. *J Agric Food Chem.* 1999; 47:3509-3517.
26. Marusek CM, Trobaugh NM, Flurkey WH, Inlow JK. Comparative analysis of polyphenol oxidase from plant and fungal species. *J Inorg Biochem.* 2005; 100:108-123.

27. Cuff ME, Miller KI, van Holde KE, Hendrickson WA. Crystal structure of a functional unit from Octopus hemocyanin. *J Mol Biol.* 1998; 278:855-870.
28. Lerch K. Amino acid sequence of tyrosinase from *Neurospora crassa*. *Proc Natl Acad Sci USA.* 1978; 75:3635-3639.